J Mater Sci (2007) 42:8172–8177
DOI 10.1007/s10853-007-1689-4

Effects of the substitution of Al for Ni on the structure and electrochemical performance of $La_{0.7}Mg_{0.3}Ni_{2.55-x}Co_{0.45}Al_x$ (x = 0–0.4) electrode alloys

Yanghuan Zhang · Dongliang Zhao · Baowei Li · Huiping Ren · Shihai Guo · Xinlin Wang

Received: 27 June 2006 / Accepted: 12 March 2007 / Published online: 9 June 2007

Abstract In order to improve the cycling stability of La–Mg–Ni system ($PuNi_3$-type) hydrogen storage alloy, Ni in the alloy was partially substituted by Al, and $La_{0.7}Mg_{0.3}Ni_{2.55-x}Co_{0.45}Al_x$ (x = 0, 0.1, 0.2, 0.3, 0.4) electrode alloys were prepared by casting and rapid quenching. The effects of the substitution of Al for Ni on the structure and electrochemical performance of the as-cast and quenched alloys were investigated in detail. The results obtained by XRD, SEM and TEM show that the substitution of Al for Ni has an inappreciable influence on the abundance of the $LaNi_2$ phase in the as-quenched alloy, while it increases the amount of the $LaNi_2$ phase in the as-cast alloys. In addition, the substitution of Al for Ni is unfavourable for the formation of an amorphous in the as-quenched alloy. The results obtained by the electrochemical measurement indicate that the cycling stabilities of the as-cast and quenched alloys are significantly ameliorated with increasing Al content. When Al content increases from 0 to 0.4, the cycle life of the as-cast and quenched (30 m/s) alloys enhances from 72 to 132 cycles and from 100 to 136 cycles, respectively.

Y. H. Zhang (✉) · D. L. Zhao · S. H. Guo · X. L. Wang
Department of Functional Material Research, Central Iron and Steel Research Institute, Beijing 100081, P.R. China
e-mails: zyh59@yahoo.com.cn; zhangyh59@163.com

Y. H. Zhang · B. W. Li · H. P. Ren
School of Material, Inner Mongolia University of Science and Technology, Baotou, Inner Mongolia 014010, P.R. China

Introduction

Intermetallic compounds for reversible hydrogen absorption/desorption have been the subject of extensive research for about 30 years. Consequently, a series of metal hydride electrode materials have been developed, such as the rare-earth-based AB_5-type alloys [1], the AB_2-type Laves phase alloys [2], the V-based solid solution alloys [3], and the Mg-based alloys [4]. Of these alloys, the AB_5-type hydrogen storage alloy has realized large-scale industrialization in many countries, such as Japan and China [5, 6]. On the basis of the development, the relevant small size Ni-MH cells have rapidly grown and gained a good share in the rechargeable battery market since the commercialization of small size Ni-MH cells in 1990. However, the rechargeable Ni-MH batteries are facing serious challenge from Li-ion cells since the Li-ion cells show higher energy density than the Ni-MH cells per unit weight or volume. The discharge capacity of currently advanced AB_5-type materials has reached 320–340 mAh/g at 0.2–0.3 C rate and room temperature. It seems to be difficult to further improve the capacity of the AB_5-type alloys as the maximum theoretical capacity of $LaNi_5$ is about 372 mAh/g. Therefore, the development of the new type of electrode alloys with higher capacity and longer cycling life is extremely important to enhancing the competition ability of the Ni-MH batteries in the rechargeable battery field. Recently, several new and good hydrogen storage alloys were reported. The most promising candidates are the La–Mg–Ni system alloys owing to their higher discharge capacities (360–410 mAh/g) and low production costs. However, the rather poor cycling stability of the La–Mg–Ni system alloys has to be further improved for commercial application. For this purpose, the worldwide researchers have carried out a lot of investigations and obtained important

results [7–10]. It is well known that the element substitution is one of the effective methods for improving the overall properties of the hydrogen storage alloys [11–13], and the manufacture technology is quite important for improving the performances of the alloys. Thus, it is expected that an appropriate amount of the substitution of Al for Ni in the La–Mg–Ni system alloy and a selected rapid quenching technique could lead to an alloy with good cycling stability. Therefore, this paper systematically investigated the effects of the substitution of Al for Ni on the structure and electrochemical performance of the $La_{0.7}Mg_{0.3}Ni_{2.55-x}Co_{0.45}Al_x$ (x = 0–0.4) electrode alloys.

Experimental

The nominal compositions of the experimental alloys are $La_{0.7}Mg_{0.3}Ni_{2.55-x}Co_{0.45}Al_x$ (x = 0, 0.1, 0.2, 0.3, 0.4). The alloys are represented by Al_0, Al_1, Al_2, Al_3 and Al_4, respectively. The alloys were melted in an argon atmosphere using a vacuum induction furnace. The purity of all the component metals (La, Ni, Co, Mg and Al) is at least 99.8%. In order to prevent the volatilization of magnesium during melting, a binary La–Mg intermediate alloy (30%Mg + 70%La) was beforehand prepared by electrolytic synthesis and a positive argon pressure of 0.1 MPa was applied. After melting, the melt was poured into a copper mould cooled by water, and a cast ingot was obtained. Part of the as-cast alloys was re-melted and quenched by melt-spinning with a rotating copper wheel. Flakes of the as-quenched alloys were obtained with different quenching rates. The quenching rate is expressed by the linear velocity of the copper wheel and the quenching rates used in the experiment are 15, 20, 25 and 30 m/s, respectively.

The phase structure and compositions of the alloys were examined by D/max/2400 X-ray diffractometer. The diffraction was performed with $CuK_{\alpha 1}$ radiation filtered by graphite. The experimental parameters for determining phase structure were 160 mA, 40 kV and 10°/min, respectively. The morphologies of the as-cast and quenched alloys were examined by SEM. The powder samples were dispersed in anhydrous alcohol for observing the grain morphology with TEM, and the crystalline state of the samples was determined by selected area electron diffraction (SAD). The granular morphologies of the electrode before and after electrochemical cycling were observed by SEM in an attempt to reveal the mechanism of the performance decay of the alloy electrodes.

Round electrode pellets of 15 mm in diameter were prepared by mixing 1 g alloy powder with fine nickel powder in a weight ratio of 1:1 together with a small amount of polyvinyl alcohol (PVA) solution as binder, and then compressed under a pressure of 35 MPa. After drying for 4 h, the electrode pellets were immersed in a 6 M KOH solution for 24 h in order to wet fully the electrodes before the electrochemical measurement.

The experimental electrodes were tested in a tri-electrode open cell, consisting of a metal hydride working electrode, a $NiOOH/Ni(OH)_2$ counter electrode and a Hg/HgO reference electrode. In order to reduce the ohmic drop between the working electrode and the reference electrode, a Luggin capillary was located close to the hydride electrode in the working electrode apartment. The electrolyte was a 6 M KOH solution. The cycling lives of the alloys electrodes were measured by an automatic galvano-static charging-discharging unit (30 °C). In each cycle, the negative electrode was charged with a constant current of 100 mA/g for 5 h, after resting 15 min, it was then discharged at 100 mA/g to a –0.500 V cut-off voltage.

Results and discussion

Effect of the substitution of Al for Ni on cycling stability

The cycling life, indicated by N, is characterized by the cycling number after which the discharge capacity of an alloy obtained with a current density of 100 mA/g is reduced to 60% of the maximum capacity. The relationship of discharge capacity versus cycling numbers of the as-cast and quenched alloys was shown in Fig. 1. The slopes of the curves of the as-cast and quenched (20 m/s) alloys obviously decreased with increasing Al content, indicating that the substitution of Al for Ni could improve the cycling stabilities of the alloys. The Al content dependence of the cycling lives of the as-cast and quenched alloys was presented in Fig. 2. The figure shows that the cycling lives of the as-cast and quenched alloys significantly increase with increasing Al content. When Al content changed from 0 to 0.4, the cycling life of the as-cast alloy increased from 72 to 132 cycles, and that of the as-quenched (30 m/s) alloy from 100 to 136 cycles. Obviously, the influence of the substitution of Al for Ni on the cycling life of the as-cast alloy is much stronger than on that of the as-quenched alloy.

Effects of the substitution of Al for Ni on microstructure

The XRD patterns of the as-cast and quenched alloys were illustrated in Fig. 3. It can seen that all of the alloys have a multiphase structure, composing of the (La, Mg)Ni_3, the $LaNi_5$ and the $LaNi_2$ phases. The substitution of Al for Ni has an inappreciable influence on the phase compositions

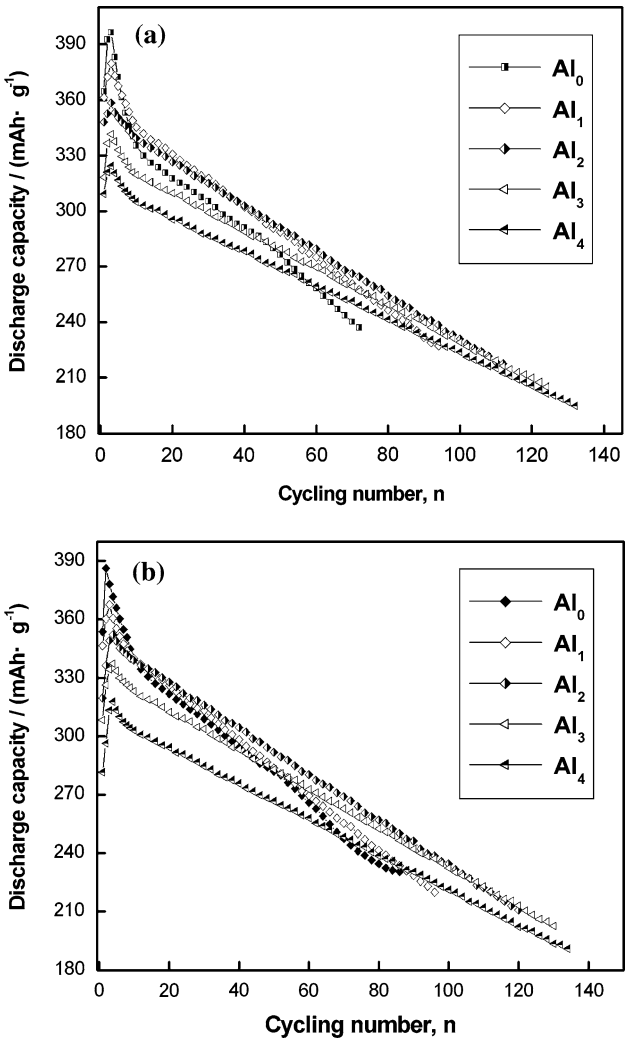

Fig. 1 The relationship between the cycle number and the discharge capacity of the alloys: (**a**) as-cast; (**b**) as-quenched (20 m/s)

of the as-cast and quenched alloys, but it obviously changes the phase abundance of the alloys. The $LaNi_2$ phase in the as-cast alloys increased with increasing Al content. So, it can be concluded by comparing the diffraction peaks of the as-cast and quenched alloys that rapid quenching increases the amount of $LaNi_2$ phase in the Al_0 alloy, but it obviously decreases the amount of $LaNi_2$ phase in the Al_3 and Al_4 alloys. The lattice parameters of the $LaNi_5$ and (La, Mg)Ni_3 main phases in the Al_0 and Al_2 alloys, which were calculated from the XRD data using a Jade5.0 software, were listed in Table 1, showing that the substitution of Al for Ni obviously increases the lattice parameters and cell volumes of the $LaNi_5$ and (La, Mg)Ni_3 main phases in the as-cast and quenched alloys, which is attributed to the atom radius of Al being larger than that of Ni. The rapid quenching leads to an increase of the *c* axis and a slight decrease of the *a* axis and cell volumes of the $LaNi_5$ and (La, Mg)Ni_3 main phases.

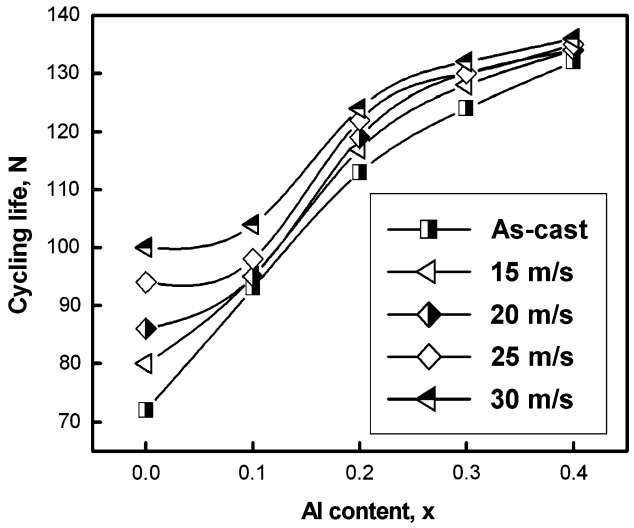

Fig. 2 The Al content dependence of the cycle life of the as-cast and quenched alloys

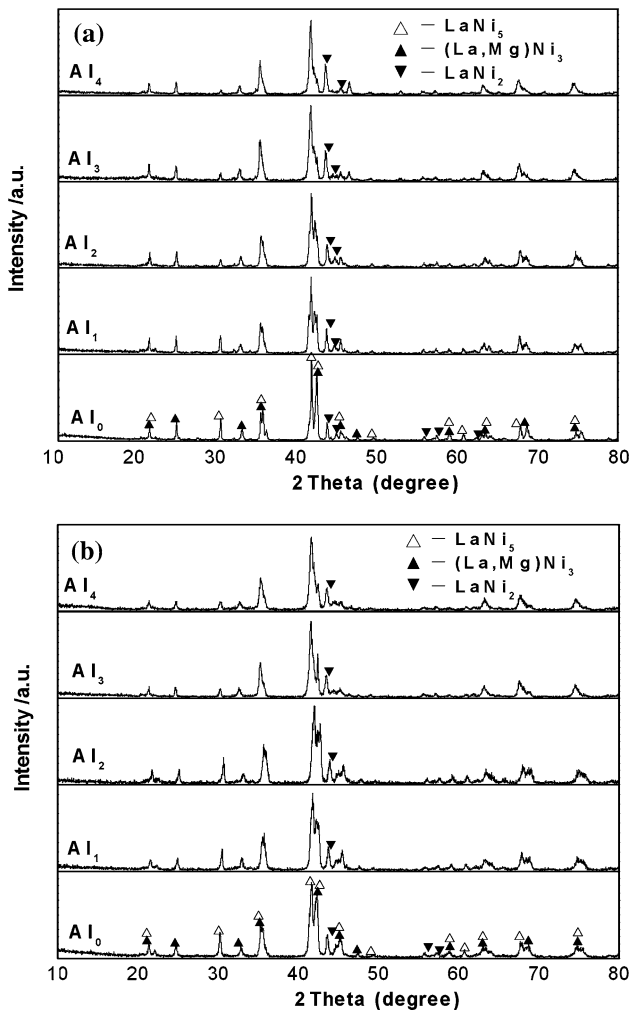

Fig. 3 The XRD patterns of the as-cast and quenched alloys: (**a**) as-cast; (**b**) as-quenched (20 m/s)

Table 1 Lattice parameters and cell volume of the $LaNi_5$ and (La, Mg)Ni_3 main phases

Conditions	Alloys	Main phases	Lattice constants		Cell volume
			a/nm	*c*/nm	V/nm^3
As-cast	Al_0	(La, Mg)Ni_3	0.5053	2.4317	0.5377
		$LaNi_5$	0.5031	0.4043	0.0886
	Al_1	(La, Mg)Ni_3	0.5058	2.4485	0.5425
		$LaNi_5$	0.5035	0.4049	0.0889
	Al_2	(La,Mg)Ni_3	0.5062	2.4642	0.5468
		$LaNi_5$	0.5038	0.4053	0.0891
	Al_3	(La, Mg)Ni_3	0.5066	2.4697	0.5489
		$LaNi_5$	0.5044	0.4059	0.0894
	Al_4	(La, Mg)Ni_3	0.5071	2.4703	0.5501
		$LaNi_5$	0.5049	0.4063	0.0897
As-quenched (20 m/s)	Al_0	(La,Mg)Ni_3	0.5046	2.4334	0.5366
		$LaNi_5$	0.5025	0.4052	0.0886
	Al_1	(La, Mg)Ni_3	0.5051	2.4487	0.541
		$LaNi_5$	0.5028	0.4057	0.0888
	Al_2	(La, Mg)Ni_3	0.5054	2.4662	0.5455
		$LaNi_5$	0.5031	0.4062	0.089
	Al_3	(La, Mg)Ni_3	0.5059	2.4701	0.5475
		$LaNi_5$	0.5035	0.4068	0.0893
	Al_4	(La, Mg)Ni_3	0.5063	2.4712	0.5486
		$LaNi_5$	0.5042	0.4071	0.896

The morphologies of the as-cast and quenched alloys observed by SEM were shown in Fig. 4. The results of energy spectrum analysis indicated that all the experimental alloys were of multiphase structure, containing both the (La, Mg)Ni_3 and the $LaNi_5$ phases. Because the amount of the $LaNi_2$ phase was small and it attaches itself to the (La, Mg)Ni_3 phase in the process of growth, it is difficult to see the morphology of the $LaNi_2$ phase. As shown in Fig. 4, the grains of the as-cast alloys are very coarse and the composition homogeneity is very poor. Compared to the morphologies of the as-cast alloys, the rapid quenching significantly refines the grains and

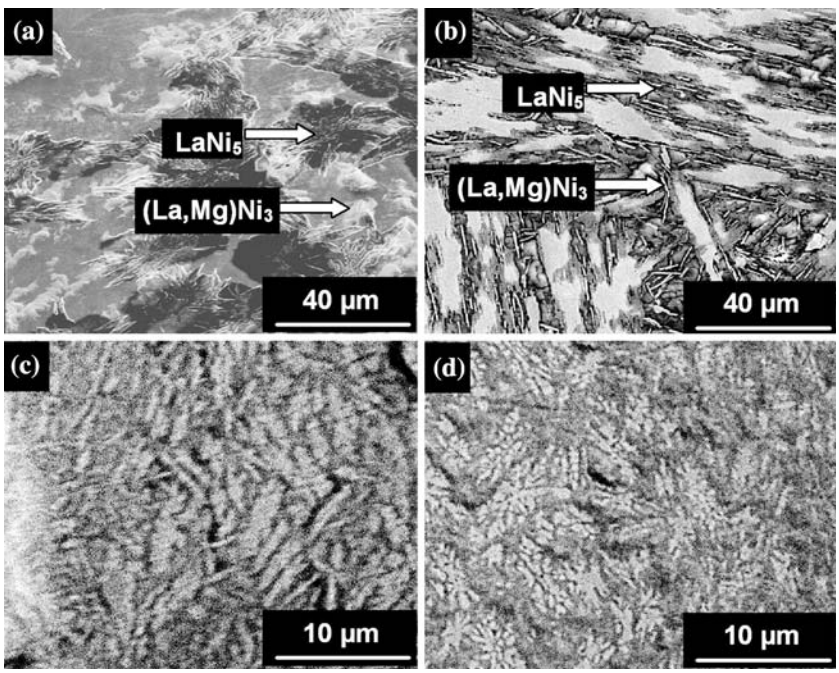

Fig. 4 The morphologies of the as-cast and quenched (20 m/s) alloys taken by SEM: (**a**), (**b**) as-cast Al_0 and Al_4 alloys; (**c**), (**d**) as-quenched Al_0 and Al_4 alloys

improves the composition homogeneity of the alloys. The grain morphologies of the as-quenched alloys are dendrite, which is different from the columnar morphology of the as-quenched AB_5-type electrode alloy [14]. The substitution of Al for Ni leads to an obvious grain refinement in the as-quenched alloys, suggesting that the substitution of Al for Ni increases the nucleation ratio and decreases the growing velocity in process of non-equilibrium crystallization of the alloys.

The morphologies and the crystalline state of the as-quenched alloys were examined by TEM, as shown in Fig. 5. The figure indicates that as-quenched (20 m/s) Al_0 alloy has a tendency of the formation of an amorphous phase but Al_2 and Al_4 alloys with the same quenching rate have a typical micro-crystal and nano-crystal structures, indicating that the substitution of Al for Ni is unfavourable to the formation of an amorphous phase in the as-quenched alloys.

The failure of the battery is characterized by the decay of the discharge capacity and the decrease of the discharge voltage [15]. The cycling stability of the electrode alloy is a crucial factor for the life of the Ni-MH battery. It is believed that the battery efficacy loss is mainly caused by negative electrode rather than positive electrode. In order to understand the mechanism of the performance deterioration of the alloy electrode, the particle morphologies of the as-quenched alloys before and after electrochemical charging–discharging cycling were observed by SEM as shown in Fig. 6. It was found that the shapes of the as-quenched alloy particles before cycling were irregular and sharp-angled with large variety of the particle sizes. After charging–discharging cycle, the particles looked less sharp and smaller. Comparing with the as-quenched AB_5-type hydrogen storage alloy, the pulverization degree of the La–Mg–Ni system alloy after electrochemical cycling was much smaller [16], and a rough and porous layer formed on

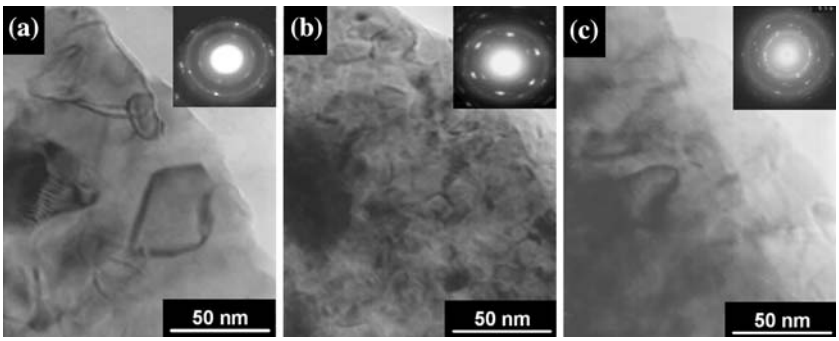

Fig. 5 The morphologies and SAD of the as-quenched (20 m/s) alloys taken by TEM: (**a**) Al_0 alloy; (**b**) Al_2 alloy; (**c**) Al_4 alloy

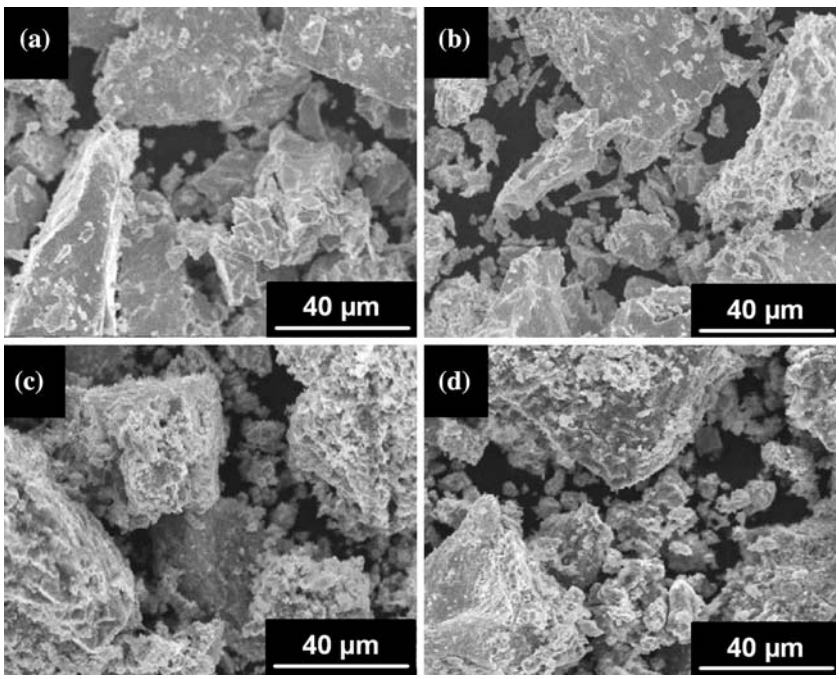

Fig. 6 The granular morphologies of as-cast alloys before and after electrochemical cycling taken by SEM: (**a**), (**b**) before cycling Al_0 and Al_2 alloys; (**c**), (**d**) after cycling Al_0 and Al_2 alloys

the surface of the La–Mg–Ni alloy, which was responsible for efficacy loss of the alloy electrode. Therefore, an effective approach to enhancing the cycling stabilities of the electrode alloys is to improve the anti-corrosion and anti-oxidation capabilities in alkaline electrolyte. The fact that the substitution of Al for Ni enhances the cycling stabilities of as-cast and quenched alloys is due to forming a dense oxide film on the alloy surface which can effectively prevent erosion of the alloy electrode in alkaline solution. In addition, the substitution of Al for Ni increases the lattice parameters and cell volumes of the alloys, which decreases the ratio of expansion/contraction of the alloy in process of the hydrogen absorption/desorption and enhances the anti-pulverization capability of the alloys. Therefore, the cycling stabilities of the alloys were improved significantly.

Conclusions

The as-cast and quenched $La_{0.7}Mg_{0.3}Ni_{2.55-x}Co_{0.45}Al_x$ (x = 0, 0.1, 0.2, 0.3, 0.4) electrode alloys have a multiphase structure, including the (La,Mg)Ni_3, the $LaNi_5$ and a small amount of the $LaNi_2$ phases. The substitution of Al for Ni engenders an inappreciable influence on the phase compositions of the as-cast and quenched alloys, but it increases the amount of the $LaNi_2$ phase in the as-cast alloys. The substitution of Al for Ni increases the lattice parameters and cell volumes of the as-cast and quenched alloys.

The substitution of Al for Ni significantly improves the cycling stabilities of the as-cast and quenched alloys. When Al content incrementally changed from 0 to 0.4, the cycling life of the as-cast alloy increases from 72 to 132 cycles, and that of the as-quenched (20 m/s) alloy from 86 to 135 cycles.

Two reasons are responsible for the efficacy loss of the La–Mg–Ni system electrode alloy. One is the pulverization during charging-discharging cycle, and the other is the corrosion and oxidation of the alloy. An effective approach to enhancing the cycling stability of the La–Mg–Ni system alloy is to improve the anti-corrosion and anti-oxidation capability of the alloy in alkaline electrolyte.

Acknowledgements This work is supported by National Natural Science Foundation of China (Grant No. 50642033), Science and Technology Planned Project of Inner Mongolia, China (Grant No. 20050205) and Higher Education Science Research Project of Inner Mongolia, China (Grant No. NJ05064).

References

1. Willems JJG, Bushow KHJ (1987) J Less Common Met 129:13
2. Ovshinsky SR, Fetcenko MA, Ross J (1993) Science 260:176
3. Tsukahara M, Kamiya T, Takahashi K, Kawabata A, Sakurai S, Shi J, Takeshita HT, Kuriyama N, Sakai T (2000) J Electrochem Soc 147:2941
4. Sun D, Enoki H, Gingl F, Akiba E (1999) J Alloys Comp 285:279
5. Wang QD, Chen CP, Lei YQ (1997) J Alloys Comp 253–254:629
6. Uehara I, Sakai T, Ishikawa H (1997) J Alloys Comp 253–254:635
7. Kadir K, Nuriyama N, Sakai T, Uehara I, Eriksson L (1999) J Alloys Comp 284:145
8. Chen J, Kurivama N, Takeshita HT, Tanaka H, Sakai T, Haruta M (2000) Electrochem Solid-State Lett 3:249
9. Kohno T, Yoshida H, F Kawashima, Inaba T, Sakai I, Yamamoto M, Kanda M (2000) J Alloys Comp 311:L5
10. Liao B, Lei YQ, Lu GL, Chen LX, Pan HG, Wang QD (2003) J Alloys Comp 356–357:746
11. Takasaki A, Sasao K (2005) J Alloys Comp 404–406:431
12. Pan HG, Liu YF, Gao MX, Li R, Lei YQ (2005) Intermetallics 13:770
13. Pan HG, Liu YF, Gao MX, Wang QD (2005) J Electrochem Soc 152(2):A326
14. Zhang YH, Dong XP, Wang GQ, Guo SH, Wang XL (2005) J Power Sources 140:381
15. Chartouni D, Meli F, Züttel Andreas, Gross K, Schlapbach L (1996) J Alloys Comp 241:160
16. Zhang YH, Wang GQ, Dong XP, Guo SH, Ren JY, Wang XL (2005) J Power Sources 148:105